Carbohydrate Polymers 112 (2014) 225–234

Contents lists available at ScienceDirect

Carbohydrate Polymers

journal homepage: www.elsevier.com/locate/carbpol

Electrosprayed inulin microparticles for microbiota triggered targeting of colon

Arvind K. Jain[1], Vishesh Sood, Meghali Bora[2], Rajesh Vasita[3], Dhirendra S. Katti*

Department of Biological Sciences and Bioengineering, Indian Institute of Technology Kanpur, Kanpur -208016, Uttar Pradesh, India

ARTICLE INFO

Article history:
Received 6 March 2014
Received in revised form 13 May 2014
Accepted 18 May 2014
Available online 6 June 2014

Keywords:
Inulin
Inulin acetate
Electrospraying
Colon targeting
Microparticles
Microbiota triggered

ABSTRACT

Inulin, a naturally occurring polysaccharide, was acetylated to make it processable by electrospraying, a facile and single step method for microparticle fabrication. Electrospraying process parameters were optimized for fabrication of spherical and monodisperse indomethacin (IDM) loaded inulin acetate (INA) microparticles. The apparent entrapment efficiency of IDM was determined to be 100%, whereas working encapsulation efficiency was estimated to be 35.39 ± 1.63%. Differential scanning calorimetry and X-ray diffraction analysis confirmed molecular dispersion of IDM in an amorphous state within the INA matrix. Finally, the results from *in vitro* release study performed in simulated gastro-intestinal fluids demonstrated that IDM was released only in simulated colonic fluid that contained inulinase. Therefore, this study demonstrates that acetylation of inulin does not alter its susceptibility to inulinase and that microparticles fabricated from INA can be developed as a colon targeting drug delivery system.

1. Introduction

Major strategies for increasing bioavailability of drugs in colon include pH sensitive and microbiota triggered drug delivery systems. These two strategies result in differential biodistribution of drug in small intestine as pH responsive systems release majority of the drug in the ileo-caecal region and microbiota triggered systems release their content reproducibly and more reliably in the transverse colon (McConnell, Short, & Basit, 2008). Microbiota-triggered colon-targeted drug delivery systems have been developed using a number of polysaccharides including chitosan (McConnell, Short, & Basit, 2008), amylose (Wilson & Basit, 2005), pectin (Jung, Arnold, & Wicker, 2013), starch (El-Hag Ali & AlArifi, 2009), guar gum (Ji, Xu, & Wu, 2007), dextran (Shrivastava & Shrivastava, 2010) and alginate (Fajardo et al., 2012). For this study we explored the use of inulin for the development of a microbiota-triggered colon targeting drug delivery system.

Inulin is a natural fructan consisting mostly of β(2-1) linked fructosyl-fructose units wherein each fructose chain is generally terminated with an α(2-1) linked glucose moiety (Niness, 1999). Inulin is not digested by the human digestive system as it lacks enzymes to cleave β(2-1) linkages in the fructose backbone. Therefore, majority of dietary inulin is not digested in the upper gastrointestinal tract. In addition to this, inulin shows a prebiotic effect as it is fermented in anaerobic conditions of colon and results in proliferation of bifidobacterium in the lower colon (Franck & De Leenheer, 2005; Vervoort & Kinget, 1996). Owing to these properties inulin has found a variety of applications in the food industry such as fat replacement, fiber supplement, prebiotic and bulk enhancer. Inulin, being a natural and bio-safe polymer with selective digestion in lower colon, was hence selected as a suitable candidate for the development of a colon targeted drug delivery system.

The current study involves the development of inulin microparticles employing a novel method of synthesis, electrospraying. Electrospraying or electrohydrodynamic atomization is a robust technique for the fabrication of micro-/nano-particles with a high degree of reproducibility (Jaworek, 2007). Electrospraying involves applying a high voltage to a polymer solution droplet. Under the influence of high voltage the polymer droplet gets charged and the arising repulsive coulombic forces overcome the surface tension of polymer solution resulting in the formation of a Taylor cone.

Abbreviations: INA, inulin acetate; IDM, indomethacin; SGF, simulated gastric fluid; SIF, simulated intestinal fluid; SCF, simulated colonic fluid.

* Corresponding author. Tel.: +91 512 2594028; fax: +91 512 2594010.
E-mail address: dsk@iitk.ac.in (D.S. Katti).
[1] Present address: School of Pharmacy, Medical Biology Center, Queen's University Belfast, Belfast-BT9-7BL, Northern Ireland, United Kingdom.
[2] Present address: School of Materials Science and Engineering, 50 Nanyang Avenue, Nanyang Technological University, Singapore 639798, Singapore.
[3] Present address: School of Life Sciences, Central University of Gujrat, Sector-30, Gandhinagar-382030, Gujrat, India.

http://dx.doi.org/10.1016/j.carbpol.2014.05.087
0144-8617/

Increasing the voltage a little higher beyond this point results in the formation of cone-jet which depending upon the polymer concentration can form a continuous fibrous structure (electrospinning) or micro-/nano-particles (electrospraying). Electrospraying is a relatively simple, single step method that allows control on particle morphology while providing high encapsulation efficiency (Arya, Chakraborty, Dube, & Katti, 2009; Seth & Katti, 2012). In our previous studies it was observed that inulin microparticles are difficult to fabricate using electrospraying (Bora, 2009). To make inulin processable by electrospraying it was modified to inulin acetate (INA). INA, owing to its hydrophobicity, is soluble in organic solvents (Wu & Lee, 2000) and as a result more concentrated and monophasic solutions of INA can be prepared in solvents which can be electrosprayed. In the current study INA was synthesized from inulin and the electrospraying parameters were optimized for fabrication of monodispersed INA microparticles loaded with a model drug indomethacin (IDM). Further, the synthesized INA microparticles were evaluated for their ability to deliver indomethacin specifically in the colon by performing *in vitro* release studies in various simulated gastrointestinal fluids. The results demonstrated that acetylation increased the processability of inulin to form microspheres by electrospraying without compromising on the colon targeting ability of the inulin.

2. Materials and methods

2.1. Materials

Inulin (from Chicory) and inulinase (sp *Aspergillus niger*, 26.7 U/mg) were procured from Sigma–Aldrich, USA. Pepsin (1:10,000, Extra pure) and pancreatin (USP specifications) were procured from Hi-Media Pvt. Ltd., India and sodium acetate, tetrahydrofuran (THF), dimethylformamide (DMF) and chloroform were procured from Merck Limited, India. Hexadeuterodimethylsulfoxide (DMSO-D6), Deuterium oxide (D_2O) and Deuterochloroform ($CDCl_3$), and acetic anhydride were procured from SD Fine-Chem Ltd., India and used as received. Indomethacin was received as a generous gift from Ideal Pharmaceuticals Pvt. Ltd., Kanpur, India. All other chemical reagents used were of analytical grade.

2.2. Synthesis of inulin acetate (INA)

INA was synthesized by modification of a previously reported method (Wu & Lee, 2000). Briefly, Inulin dissolved in dimethylformamide (DMF) was esterified by acetic anhydride in presence of 0.05% sodium acetate, the catalyst, at 40 °C for 24 h. Reaction was carried out in a rotary flask evaporator (Rotary Vacuuma, Perfit India) under vacuum to protect the reactants and products from oxygenation and hydration. After reaction INA was collected by its precipitation with deionized water; washed twice and dried in a vacuum oven at 40 °C for 6–8 h.

2.3. Characterization of inulin and INA

The degree of polymerization of the procured inulin was confirmed by ^{13}C Nuclear magnetic resonance (NMR) spectroscopy. Whereas, the synthesized INA was characterized by Fourier transform infrared spectroscopy (FTIR), ^{1}H NMR and gel permeation chromatography (GPC).

2.4. FTIR spectroscopy

The chemical structure of inulin and INA, and the qualitative validation of acetylation of inulin was studied using FTIR spectroscopy. Samples were lyophilized for 24 h before being pelleted in KBr to record spectra from 400 to 4000 cm^{-1} using a FTIR spectrometer, Vertex -70 (Bruker Optik GmBH, Germany).

2.5. NMR spectroscopy

^{1}H NMR and ^{13}C NMR spectra were recorded using ECX-500 Delta-2 spectrometer (JEOL, Japan) operating at a frequency of 500 MHz and 125 MHz respectively. For spectral recording inulin was dissolved in D_2O and INA was dissolved in $CDCl_3$, whereas, for comparative studies both samples were analyzed in DMSO-D_6.

The degree of polymerization of native inulin was estimated from its ^{13}C NMR spectrum by taking the ratio of peak integral values of carbons in fructose units to the peak integration values of the corresponding carbons in the glucose unit using Eq. (1) (Franck & De Leenheer, 2005).

Whereas, the degree of acetylation of INA was estimated from its ^{1}H NMR spectrum by using relative change in the ratio of integrals of resonance peaks at ~2 and 3.5–5.5 ppm corresponding to methyl proton of acetate (acetylation) and protons of fructose skeleton (native inulin) respectively using Eq. (2) and then determining the percentage of acetyl modified hydroxyl groups present in INA using Eq. (3). The integrals of resonance peak were divided by number of protons present in each moiety.

$$\text{Degree of polymerization} = \frac{\text{Absorbance of skeletal carbon of fructose}}{\text{Absorbance of respective carbon in glucose unit}} \quad (1)$$

$$\text{Acetyl group per fructose unit} = \frac{(A_2/3)}{(A_{3.5-5.5}/7)} \quad (2)$$

$$\text{Degree of Acetylation} = \frac{\text{Acetyl group per fructose unit}}{\text{Number of OH group per Fructose unit}} \times 100 \quad (3)$$

2.5.1. Gel Permeation Chromatography (GPC)

The INA sample was characterized for molecular weight and polydispersity using GPC instrument (Waters, USA) equipped with a refractive index detector and a Styragel® column (HR2/HR4 THF). The mobile phase used was tetrahydrofuran (THF) and was maintained at a flow rate of 1 mL/min. Temperature of the column and detector was maintained at 40 °C. Average molecular weight of INA samples was calculated by measuring area under the curve for INA chromatogram and comparing it with a series of polystyrene molecular weight standards.

2.6. Fabrication and optimization of blank INA microparticles by electrospraying

Electrospraying apparatus used for the fabrication of INA microparticles was assembled in-house (Arya, Chakraborty, Dube, & Katti, 2009). Briefly, a solution of INA in chloroform was ejected through a blunt-end stainless steel needle under a constant flow rate of 0.2 mL/h using an automated syringe pump (11 plus, Harvard Apparatus, USA). A high-voltage electric field was generated between the needle and the collector electrode using a high voltage supply unit (Glassman High Voltage Inc., USA). The electrosprayed microparticles were collected on an aluminum foil placed on a grounded collector electrode. The electrospraying parameters were optimized by varying one parameter at a time (Table 1) with the objective of obtaining spherical and monodisperse microparticles. The morphology of as-prepared microparticles was studied by

Table 1
Experimental design for one parameter at a time optimization of electrospraying for fabrication of INA microparticles.

Study Parameters		Constant Parameters			
Parameter	Range	Needle gauge (G)	Electrospraying voltage (kV)	Electrospraying distance[a] (cm)	Polymer concentration (%, w/v)
Needle gauge (G)	20, 22, 24, 26	–	20	20	15
Electrospraying voltage (kV)	15, 20, 25, 30	24	–	20	15
Electrospraying distance (cm)[a]	18, 20, 22, 24	24	20	–	15
Polymer concentration (%, w/v)	10, 12, 15, 17	24	20	20	–

[a] Distance between needle tip and collector electrode

micrographs obtained with the Scanning Electron Microscope (SEM, FEI Quanta 200).

2.6.1. Formulation of Indomethacin (IDM) loaded INA microparticles

10% (w/w) IDM was added to the INA solution in chloroform to formulate IDM loaded INA microparticles. The process was optimized for generation of spherical IDM loaded INA microparticles by varying the electrospraying voltage and electrospraying distance. The needle gauge and polymer concentration were used without change as-optimized for the fabrication of blank INA microparticles.

2.7. Characterization of IDM loaded INA microparticles

2.7.1. Morphology

The surface morphology and size of IDM loaded INA microparticles were characterized by scanning electron microscopy (SEM, FEI Quanta 200). Samples were sputter coated with gold and were observed at a working distance of 10 mm and an accelerating voltage of 20 kV.

2.7.2. Drug entrapment efficiency and loading capacity

The entrapment efficiency of IDM loaded INA microparticles was determined after washing INA microparticles with phosphate buffered saline (PBS, pH 7.4) to get rid of loosely surface associated IDM. Briefly, microparticles were washed twice with PBS 7.4 either by vortexing for 30 min or incubating in PBS 7.4 for 1 h in a rotary bath incubator at 75 rpm. The washed microparticles were collected by centrifugation at 15,000 × *g* for 10 min and were lyophilized (Alpha 1-2 LD lyophilizer, Christ, Germany). A fixed amount of dried microparticles was dissolved in chloroform followed by quantification of IDM by UV spectroscopy (UV 1, Thermo Scientific, USA). The absorbance peaks of IDM in chloroform were found to be at 266 and 320 nm (Supplementary Fig. S1). The absorbance peak at 320 nm was used for the quantification of IDM spectrophotometrically as at this wavelength inulin acetate does not show any interference. The amount of surface-associated IDM washed from the microparticles was also estimated by analyzing the supernatant after centrifugation which enabled the validation of entrapment efficiency of IDM in INA microparticles. Further, IDM loading capacity in INA microparticles was determined by calculating the amount of drug present as weight-by-weight (w/w) percentage of microparticles.

$$\text{Percentage Entrapment Efficiency} = \frac{\text{Amount of drug quantified}}{\text{Amount of drug used}} \times 100 \quad (4)$$

$$\text{Percentage loading capacity} = \frac{\text{Amount of drug quantified (mg)}}{\text{Amountof microparticles (mg)}} \times 100 \quad (5)$$

2.8. X-ray diffraction spectroscopy

The crystallinity of IDM encapsulated in microparticles was determined by X-ray diffraction spectroscopy. XRD spectra were obtained using an ARL X'TRA X-ray diffractometer (Thermo Electron Corporation, Switzerland) working at 25 °C over a 2θ range of 7–40° at a rate of 3°/min (step 0.05°) using CuKα radiation.

2.9. Differential Scanning Calorimetry (DSC)

DSC analysis was performed on a Pyris 6 Differential Scanning Calorimeter (PerkinElmer, USA) under nitrogen atmosphere (50.0 mL/min), using approximately 5 mg of sample contained in an aluminum pan, and a heating rate of 10 °C/min for a range of 30–200 °C. The DSC cell was calibrated with indium (melting point 156 °C) and zinc (melting point 419.4 °C) standards.

2.10. In vitro drug release study

INA microparticles were evaluated for their efficacy for targeting and releasing drug in the colon by a three-step *in vitro* release study, step 1 in simulated gastric fluid (SGF), step 2 in simulated intestinal fluid (SIF) and step 3 in simulated colonic fluid (SCF) in order to simulate gastrointestinal (GI) conditions. SGF (pH 1.2, pepsin 0.32%, w/v) and SIF (pH 6.8, pancreatin 1%, w/v) were prepared according to United State Pharmacopoeia 25 NF 20; whereas, SCF was prepared by dissolving 5 U/mL inulinase in phosphate buffer (pH 6.8).

IDM encapsulated INA microparticles were washed and loaded into a dialysis bag having a molecular weight cutoff of 3500 Da (Sigma–Aldrich, USA). The INA microparticles loaded dialysis bag was first incubated in SGF for 2 h then in SIF for 4 h followed by SCF for 18 h. As IDM shows pH dependent solubility, its solubility in all three GI fluids was determined a priori to ensure that sink conditions were maintained throughout the experiment. At specific time points 1 mL of sample was withdrawn and the dialysis bag was replenished with fresh buffer. The withdrawn samples were analyzed by UV–vis spectroscopy at 320 nm to quantify the amount of IDM released. Cumulative percent IDM released was plotted as a function of time (in hours) to arrive at the release profile of the developed formulation under simulated gastrointestinal conditions.

3. Results and discussion

3.1. Characterization of inulin and INA

3.1.1. FTIR spectroscopic analysis of inulin and INA

A wide peak of hydroxyl group at 3369 cm^{-1}, C–H vibration at 2929 cm^{-1}, C–O–H bending at 1438 cm^{-1} and peaks corresponding to the tetrahydrofuran ring of fructose at 1031 cm^{-1} were observed in the FTIR spectrum of inulin (Fig. 2). Peaks similar to the functionalities observed in inulin were observed in the FTIR spectrum of INA at 3488, 2954, 1434 and 1039 cm^{-1} respectively. The small shift

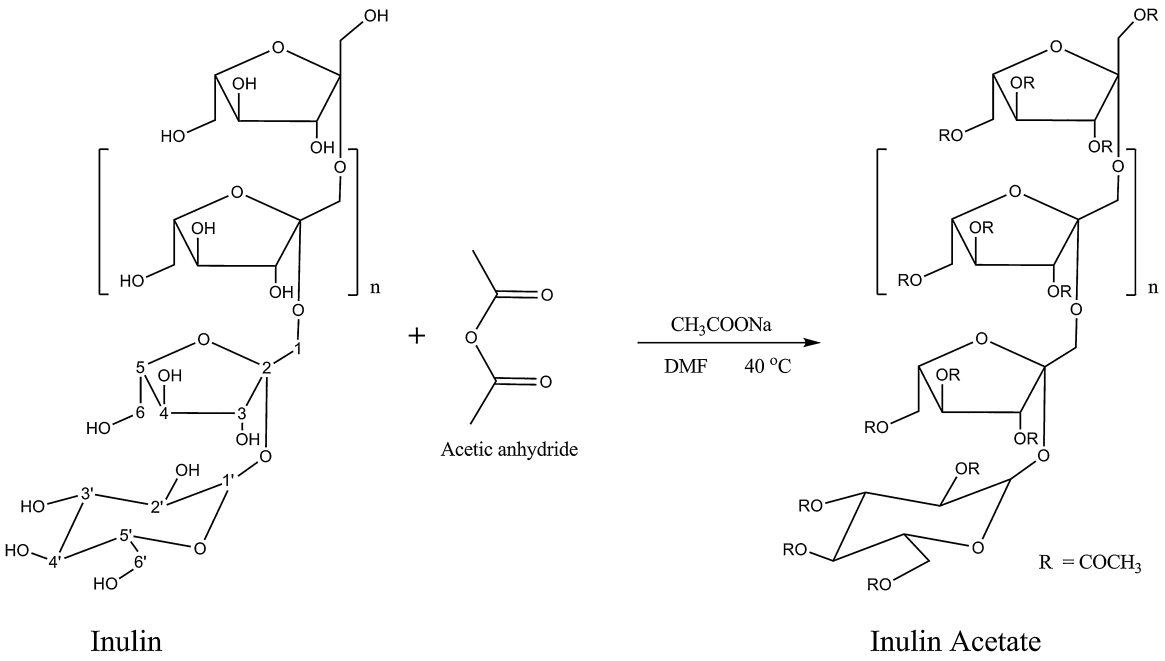

Fig. 1. Schematic representation of synthesis of inulin acetate.

observed in peaks was attributed to decreased hydrogen bonding and presence of increased number of C–H bonds due to addition of $-CH_3$. In addition to these peaks, the INA spectrum also had a carbonyl peak at 1745 cm^{-1}, a $-CH_3$ bending peak at 1373 cm^{-1} and a –C–O bending peak at 1236 cm^{-1} which correspond to the acetyl ($-COCH_3$) group in INA. The presence of the acetyl group while maintaining all the other characteristic peaks of inulin confirmed the successful acetylation of inulin to INA.

3.1.2. Gel permeation chromatography

GPC was performed to determine the molecular weight and polydispersity of synthesized INA. Number average molecular weight (M_n) and weight average molecular weight (M_w) of INA was estimated to be 4599 and 5287 Da respectively. The polydispersity (M_w/M_n) of INA was calculated to be 1.15. The characteristic peaks of inulin observed in the FTIR analysis of INA combined with its low polydispersity indicated that inulin was not adversely affected during the acetylation reaction. Also, the observed unimodal mass distribution (Supplementary Fig. S2) indicated absence of any unacetylated inulin in the final product and as a consequence uniformity of acetylation reaction.

3.1.3. NMR studies of inulin and INA

Degree of polymerization of inulin: Glucose containing inulin is composed of repeated fructose units and one terminal glucose unit linked through β (2-1) glycosidic linkages (Fig. 1).

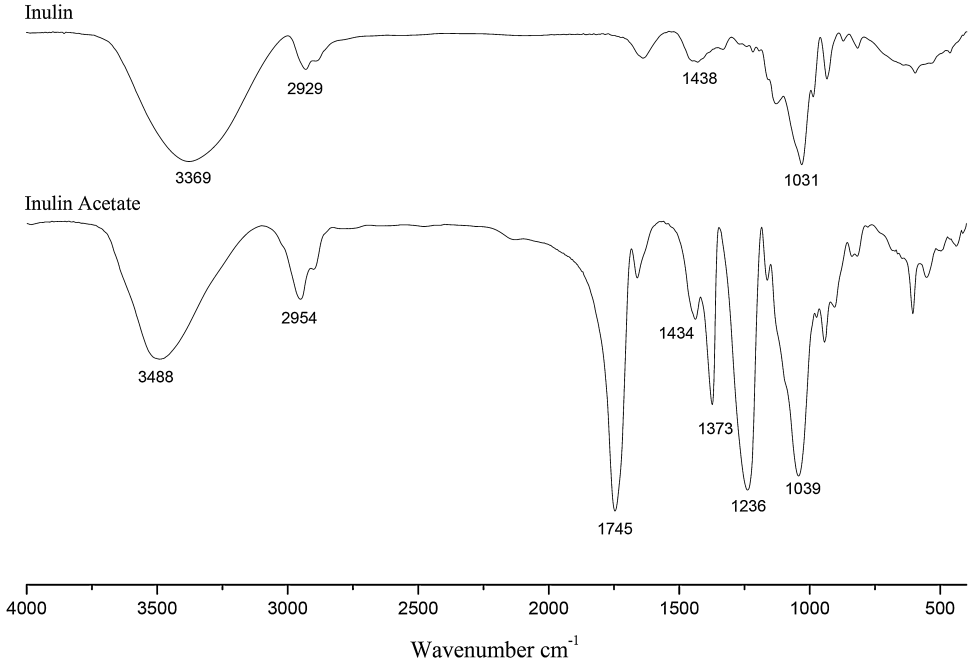

Fig. 2. FTIR spectra showing characteristic peaks of inulin and INA.

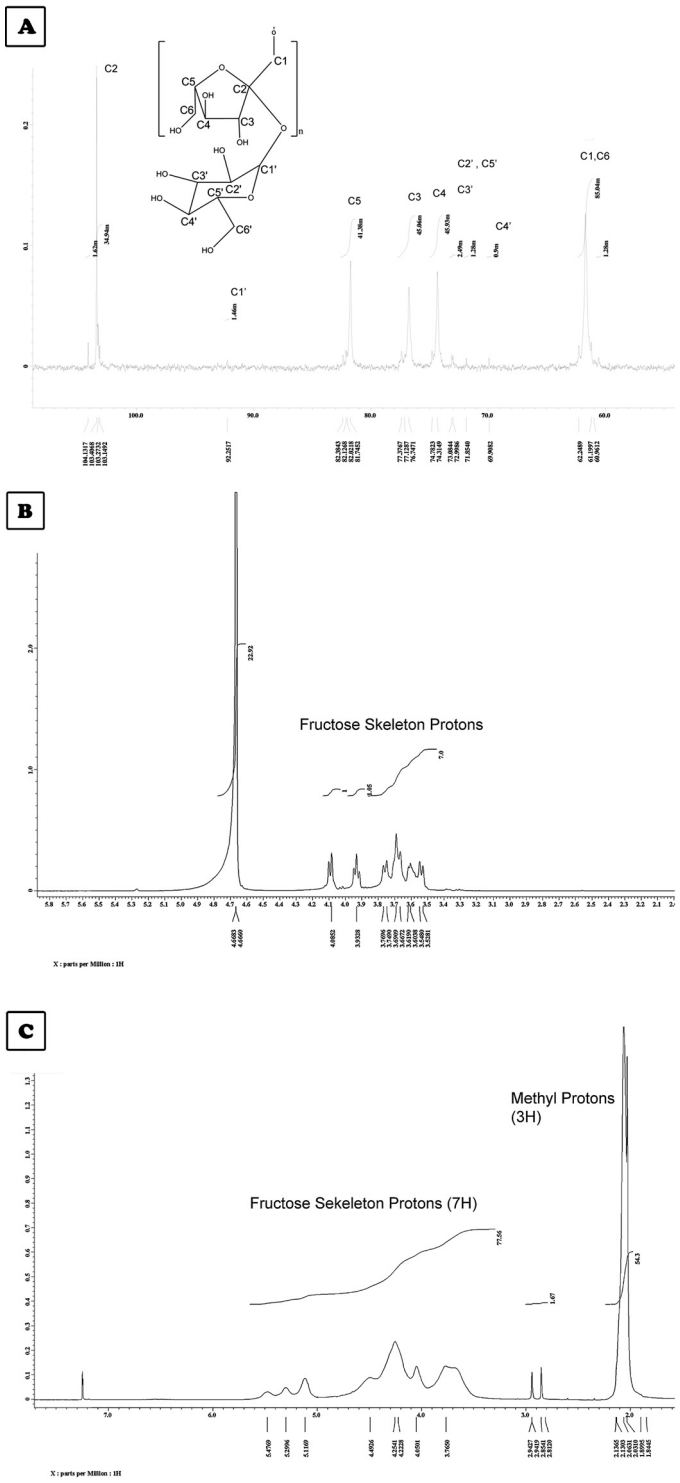

Fig. 3. NMR characterization of inulin and INA. (A) ^{13}C NMR spectrum of inulin; (B) ^{1}H NMR spectrum of inulin; (C) ^{1}H NMR spectrum of INA.

Inulin used in this study had a fructose:glucose ratio of more than 25. The degree of polymerization (DPn) in case of glucose containing inulin is defined as the ratio of fructose units to the glucose units. DPn of native inulin was determined by ^{13}C NMR spectroscopy wherein two classes of peaks were observed (Fig. 3A). The first class contained prominent peaks for C1–C6 carbons ($\delta_{C1} \sim 62$ ppm, $\delta_{C2} \sim 103$ ppm, $\delta_{C3} \sim 77$ ppm, $\delta_{C4} \sim 74$ ppm, $\delta_{C5} \sim 82$ ppm and $\delta_{C6} \sim 62$ ppm) of fructose ring due to fructose repeat units, whereas, the second class comprised of very weak peaks for C1′–C6′ ($\delta_{C1'} \sim 92$ ppm, $\delta_{C2'} \sim 72$ ppm, $\delta_{C3'} \sim 73$ ppm, $\delta_{C4'} \sim 70$ ppm, $\delta_{C5'} \sim 73$ ppm and $\delta_{C6'} \sim 62$ ppm) due to reduced presence of terminal glucose units (Fig. 3A). Degree of polymerization was determined as the ratio of integral value of a carbon atom of fructose ring to integral value of the corresponding carbon atom in the glucose ring (Fig. 3A). The DPn of inulin was estimated to be around 30 which corroborates with the supplier's specification of greater than 25.

Degree of acetylation of INA: The efficiency of acetylation reaction was determined by degree of acetylation of INA. ^{1}H NMR spectrum of INA was used for measuring the peaks specific to fructose rings of inulin and methyl group of acetyl side chain. Characteristic peaks corresponding to the skeleton protons of fructose ring in the range of 3.5–5.5 ppm were observed in the ^{1}H NMR spectra of both inulin and INA (Fig. 3B and C). In contrast, methyl side chain of acetyl group showed a distinct and sharp peak at ~2 ppm in the ^{1}H NMR spectrum of INA only. The number of acetyl groups per unit of fructose was determined by the ratio of integrals of these two peaks and the degree of acetylation was calculated as the percentage of the number of acetyl substituted hydroxyl groups present in fructose units. Number of acetyl groups per fructose unit and degree of acetylation was found to be 1.618 and 54% respectively.

3.2. Fabrication and optimization of blank INA microparticles

To determine the optimal range of electrospraying parameters for fabrication of monodisperse and spherical INA microparticles, the method of single parameter optimization was used. Scanning electron microscopy was used to study the size and morphology of INA microparticles. Fig. 4 shows the scanning electron micrographs of INA microparticles fabricated during the optimization of electrospraying parameters.

3.3. Effect of needle gauge

Effect of needle gauge on microparticle fabrication using electrospraying was studied for the following range of needle gauges: 18, 20, 22, 24 and 26G. Below needle gauge of 18G sputtering was observed with no microparticles being formed. Electrospraying with 18G and 20G needles resulted in sputtering along with the formation of microparticles (for results obtained using 18G needle see supplementary Fig. S3A). This sputtering was attributed to higher effective flow rate due to the relatively larger internal diameters of needles with smaller gauges (≤20 G). Increasing the needle gauge to 22 G resulted in fabrication of microparticles without sputtering (Fig. 4, first row). Electrospraying with 24G needle resulted in fabrication of monodispersed spherical microparticles. Increasing the needle gauge to 26 G resulted in increase in polydispersity of microparticles size. For needles with needle gauge greater than 22 G a stable jet of polymer solution formed resulting in generation of microparticles without sputtering. Based on these results, 24 G was selected as the optimum needle gauge for further experiments.

3.3.1. Effect of electrospraying distance

Electrospraying distance, the distance between tip of the needle and collector electrode was the next parameter for optimization. Electrospraying was performed at distances ranging from 18 to 24 cm with an increment of 2 cm. Distances ≤18 cm resulted in aggregation of formed microparticles (Supplementary Fig. S3B). This was attributed to incomplete evaporation of solvent resulting in the deposition of wet microparticles. However, increasing the distance to 20 cm resulted in the fabrication of microparticles with reduced aggregation along with good homogeneity in size (Fig. 4, second row). With further increase in distance (>20 cm) an increase in the polydispersity of microparticle size was observed. Furthermore, at higher electrospraying distance (24 cm) a decrease in the

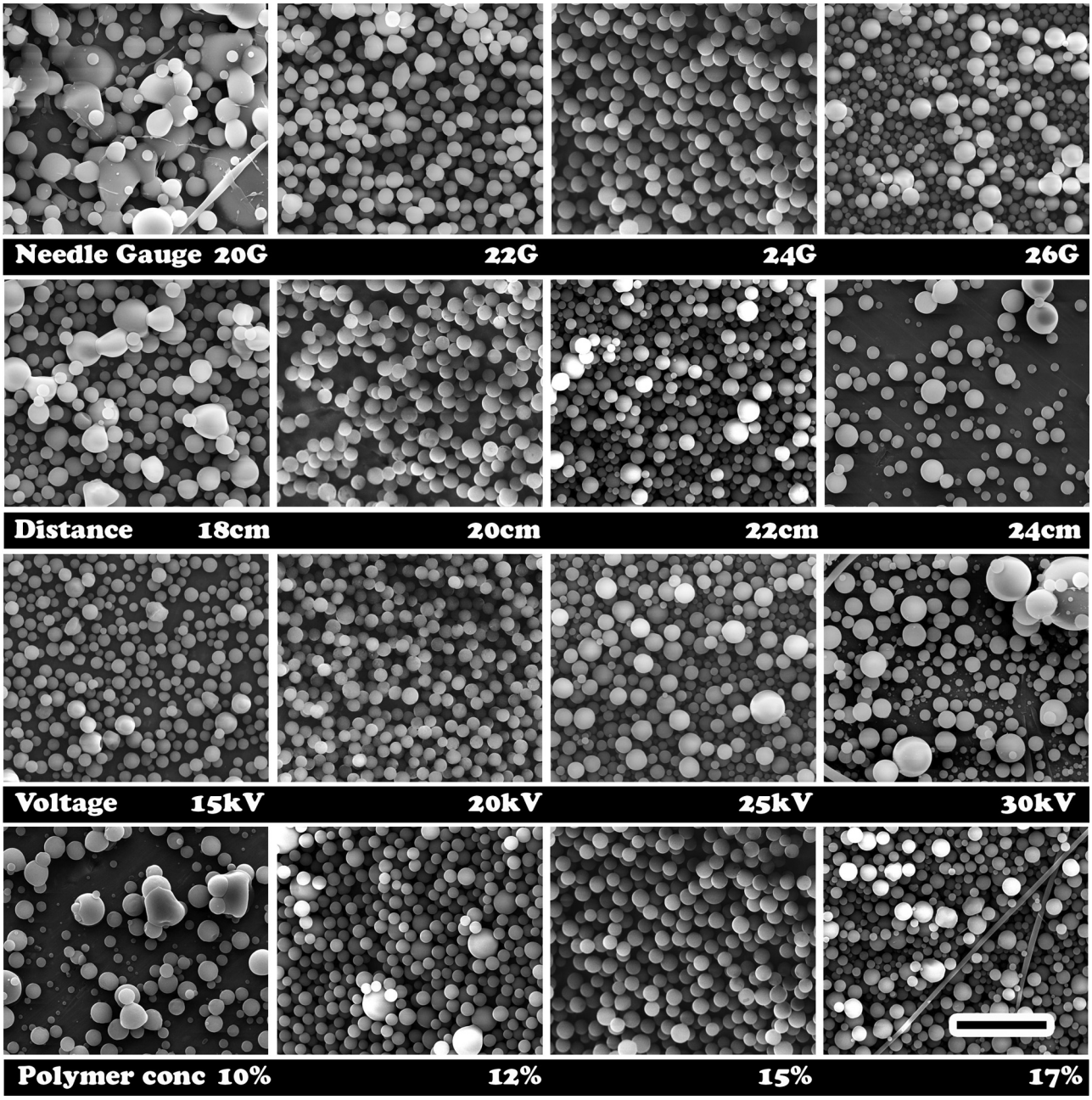

Fig. 4. Optimization of electrospraying parameters for fabrication of INA microparticles: first row: effect of needle gauge; second row: effect of electrospraying distance (tip to electrode distance); third row: effect of electrospraying voltage; fourth row: effect of polymer concentration. (All images have a magnification of 5000× and scale bar = 20 μm.)

amount of microparticles deposition was also observed. During the process of electrospraying, the polymer jet ejected from the tip of the needle breaks due to instabilities generated by the high voltage. In the given set of conditions increasing the distance resulted in a decrease in effective electric field per unit distance and thus caused a breakdown of cone-jet generating droplets of irregular size. There is also the possibility of secondary breaking (splitting of droplets) if larger volume microdroplets are formed during the first jet breaking in case of longer distances. We speculate this to be the probable cause of fabrication of polydisperse microparticles at higher electrospraying distances (≥22 cm). In addition to increased polydispersity, decreased effective electric field is known to reduce the rate of particle deposition (Arya, Chakraborty, Dube, & Katti, 2009). Based on these studies, electrospraying distance of 20 cm was selected as the optimal distance and was used for further experiments.

3.3.2. *Effect of electrospraying voltage*

The next set of experiments was conducted to optimize electrospraying voltage. Range selected for optimization was 15–30 kV with an increment of 5 kV. At 15 kV low microparticles deposition was observed while increasing the voltage to 20 kV resulted in fabrication of spherical microparticles with good amount of deposition (Fig. 4, third row). On further increasing the voltage to 25 and 30 kV there was an increase in polydispersity of formed INA microparticles. At higher voltages (>30 kV) fibrous structures were also observed along with microparticles (Supplementary Fig. S3C). Voltage is an important parameter of electrospraying as high

voltage is required for formation of Taylor cone and an optimum voltage is required for the formation of monodispersed spherical microparticles. Below this optimum value of voltage, the electrospraying process exhibits decreased rate of deposition because of lack of effective drawing force per unit length of travel. However, higher voltage results in increase in droplet diameter near needle and breaking of cone-jet into multi-jets leading to fiber formation and generation of polydispersed microparticles (Bagheri-Tar, Sahimi, & Tsotsis, 2007; Jaworek & Krupa, 1999). This was corroborated by results obtained with electrospraying of INA at varying voltage. Based on these results 20 kV was selected as optimal voltage and was used for further experiments.

3.3.3. Effect of polymer concentration

For these experiments, a range of polymer concentrations including 10, 12, 15 and 17% (w/v) were studied (Fig. 4, fourth row). Sputtering was observed at concentrations lower than 10% (w/v) (results not shown). This sputtering was attributed to increase in solvent to polymer ratio in micro-droplets formed during the process of electrospraying. The presence of excess solvent leads to deposition of wet microparticles. When the polymer concentration was increased to 12% (w/v), it was observed that smaller sized microparticles were formed predominantly along with a small number of larger sized microparticles. INA microparticles formed at polymer concentration of 15% (w/v) were monodispersed and spherical. Further increase in concentration resulted in the formation of polydispersed microparticles along with fibrous structures. This was probably due to the viscous forces present at higher polymer concentration that helped in overcoming Rayleigh forces which are essential for the breakage of jet and consequential formation of microparticles (Bock, Woodruff, Hutmacher, & Dargaville, 2011). Based on these studies, 15% (w/v) concentration of INA was selected as the optimal concentration for the fabrication of blank INA particles. The results of the optimization study are as shown in

3.4. Formulation of IDM loaded INA microparticles

To prepare IDM loaded INA microparticles, 10% (w/w) IDM with respect to the polymer weight was added to the solution of INA in chloroform. For initial experiments the optimal parameters for INA microparticle synthesis were used. Loading of IDM caused changes in the polymer solution resulting in changes in morphology of INA microparticles. Therefore, the synthesis procedure for IDM loaded nanoparticles was optimized further. Needle gauge and polymer concentration were kept constant at 24 G and 15% (w/v) and different sets of electrospraying distance and voltage were studied (Supplementary Fig. S4). On the basis of these experiments, final variables optimized for the formulation of IDM loaded microparticles were found to be: Needle gauge 24 G, electrospraying distance 24 cm, electrospraying voltage 20 kV, polymer concentration 15% and drug–polymer ratio 10% (w/w) (Table 2). Surface morphology of the IDM loaded microparticles was studied by scanning electron microscopy (Fig. 5A). It was observed that the IDM loaded INA microparticles were spherical in shape and around 3 μm in diameter.

3.5. Characterization of IDM loaded INA microparticles

3.5.1. Entrapment efficiency and loading capacity

Electrospraying, by virtue of being a single step fabrication method, allows for relatively higher entrapment of drugs in the microparticles. As a significant amount of drug remains surface adsorbed rather than being entrapped in the polymer matrix, the entrapment efficiency was determined after washing the microparticles twice with PBS. Microparticles were freeze-dried after washing and entrapped drug was quantified by dissolving the freeze-dried microparticles in chloroform and measuring the absorption of IDM at its absorption maxima (320 nm). The working percent entrapment efficiency of inulin microparticles was found to be $35.39 \pm 1.63\%$ ($n = 6$) and percent-loading capacity was calculated as $3.54 \pm 0.16\%$ ($n = 6$). The entrapment efficiency of the unwashed microparticles was found to be 100% indicating that there was no drug loss during the process of electrospraying. Using this fact the amount of IDM released after washing with PBS was quantified and used to cross validate the working entrapment efficiency.

3.5.2. Differential scanning calorimetry

DSC was performed to study the thermal properties of the polymers. A significant decrease in the melting temperature (T_m) was observed due to the acetylation. Tm for inulin was recorded to be 173.22 °C while that of INA was 81.62 °C. These results are in agreement with previous reports (Poulain et al., 2003; Wu & Lee, 2000).

DSC analysis was also performed to assess the molecular phase and dispersion of IDM inside the INA microparticles. A homogenous dispersion at a molecular level and absence of crystalline form of drug in loaded microparticles ensures the stability of the formulation with a predictable release profile of the drug (Karavas, Georgarakis, Sigalas, Avgoustakis, & Bikiaris, 2007). DSC thermogram of IDM showed an endothermic melting peak at 162.26 °C, which corresponds to its melting point (Tm) and the sharpness of the peak was attributed to its crystalline nature (Fig. 5B). The Tm for INA microparticles was found to be 79.71 °C, which was slightly less than the Tm of INA, 83.62 °C. Based on the similarity of the thermograms of blank and IDM loaded INA microparticles and the absence of an endothermic peak for Tm of IDM in the loaded microparticles, it was concluded that IDM was present in the amorphous phase and was homogenously dispersed in the INA microparticles.

3.5.3. X-ray diffraction spectroscopy

The results of DSC analysis that indicated the presence of drug in amorphous phase inside the microparticles was validated by X-ray diffraction studies. Crystallization of the drug within the polymer matrix causes slower drug release as higher activation energy is required to dissolve crystals as compared to amorphous powder (Wu, Zhang, & Watanabe, 2011). Inulin showed a crystalline state whereas INA was observed to be more in an amorphous state (Fig. 5C). The diffractogram of IDM showed peaks at 11.6°, 17.05°, 19.6°, 21.8°, 24°, 26.6° and 29.3°. Most of these peaks were also observed in the diffractogram of physical mixture of IDM and INA (1:10). However, these peaks were absent in the diffractogram of IDM loaded microparticles. These results validated DSC results in establishing that IDM did not recrystallize in the INA microparticles and was molecularly dispersed in the INA matrix inside the microparticles.

3.6. In vitro drug release

The efficiency of the developed microparticles to serve as a colon targeted drug delivery system was evaluated by performing an *in vitro* drug release study. For successful colon targeting a delivery system must overcome gastrointestinal (GI) barriers which include acidic pH of the stomach and the small intestine. The release of IDM from IDM loaded INA microparticles was studied using an appropriate sequence and duration of exposure of simulated gastric fluids to evaluate the colon targeting efficacy of INA microparticles. These conditions included incubation in simulated gastric fluid (SGF, pepsin enzyme and pH 1.2) for two hours, followed by incubation in simulated intestinal fluid (SIF, pancreatin enzyme, pH 6.8) for four hours and finally incubation in simulated colonic fluid (SCF, inulinase enzyme, pH 6.8) for eighteen hours. These time points

Table 2
Electrospraying parameters optimized for fabrication of blank and IDM loaded INA microparticles.

Electrospraying parameter	Blank INA microparticles		Optimal value for IDM loaded INA microparticles
	Range	Optimal value	
Needle Gauge (G)	18–26	24	24
Electrospraying Distance (cm)	18–24	20	24
Electrospraying Voltage (kV)	15–30	20	20
Polymer concentration (%, w/v)	10–17	15	15

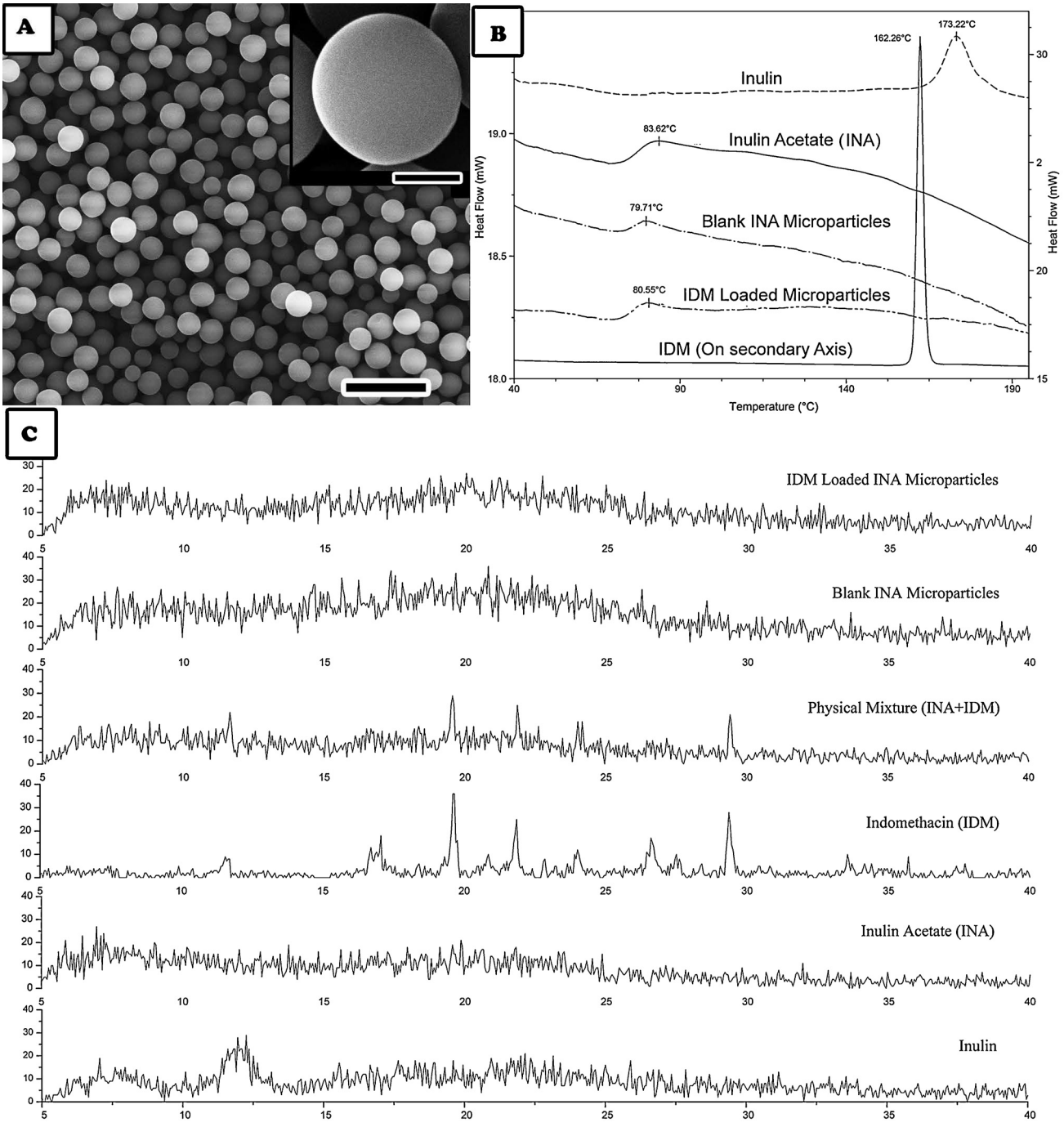

Fig. 5. Characterization of IDM loaded INA microparticles. (A) Scanning electron micrograph of INA microparticles (magnification 5000×, scale bar = 10 μm), Inset shows a single microparticle (magnification 33000×, scale bar = 1.5 μm). (B) DSC thermograms depicting melting temperature (T_m) of inulin, INA, blank microparticles, IDM loaded microparticles and IDM (IDM is plotted on secondary axis for the convenience of data presentation). (C) X-ray diffraction patterns of inulin, INA, IDM, physical mixture of IDM and INA (1:10 ratio), blank microparticles and IDM loaded microparticles.

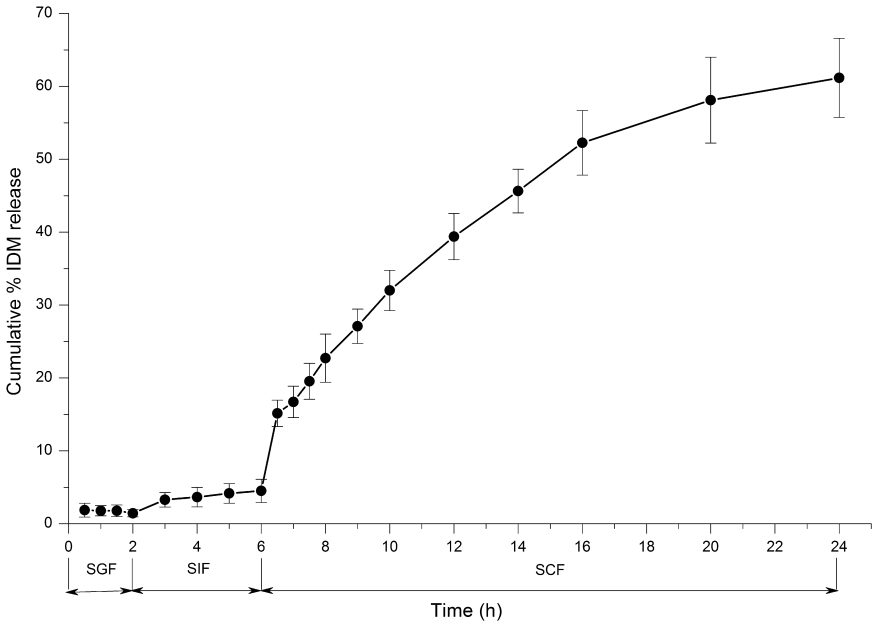

Fig. 6. *In vitro* release kinetics of IDM from INA microparticles under simulated GI conditions. (IDM – indomethacin; SGF – simulated gastric fluid; SIF – simulated intestinal fluid; SCF – simulated colonic fluid).

were selected in accordance to movement of food in GI tract (Davis, Hardy, & Fara, 1986). Inulin is not digested by any human digestive enzyme as carbohydrate back-bone in inulin is linked by β(2-1) linkage and is thus only fermented by colonic microbiota which release an enzyme called inulinase that can cleave these β(2-1) linkages (Niness, 1999). Hence inulinase was added to the SCF to mimic these colonic conditions.

The release profile of IDM from INA microparticles under the aforementioned conditions was as shown in Fig. 6. The results of the *in vitro* IDM release study indicated that the microparticles did not release an appreciable amount of IDM during the first 2 h of incubation in SGF. Hence, these microparticles were considered to be stable under low pH and harsh conditions of stomach. On transferring these microparticles to the SIF a small amount of drug (<5%) was released and the amount of released IDM did not change significantly during the four hours of incubation. On changing the incubating buffer to SCF a sharp increase in the amount of IDM released from INA microparticles was observed. Approximately 61% of the loaded IDM was released from INA microparticles after 18 h of incubation in SCF. To ascertain the role of inulinase in the release of IDM from INA microparticles, a release study was also conducted in SCF in the absence of inulinase. The results (Supplementary Fig. S5) showed approximately 5% IDM release after 48 h of incubation. These results indicate that IDM was released from INA microparticles only in SCF containing inulinase.

Mathematical modelling of the IDM release kinetics (Supplementary Fig. S6 and Supplementary Table 1) showed that drug release profile fits well to Higuchi and Korsmeyer-Peppas models of drug release with r^2 values of 0.991 and 0.986 respectively (Costa & Sousa Lobo, 2001). Both Higuchi and Korsmeyer-Peppas models suggest that the drug was released due to diffusion. The slope of the plot for Korsmeyer-Peppas model was 0.52 which indicated that the diffusion was anomalous and the overall diffusion was a combination of both Fickian-diffusion (diffusion of solute from higher concentration to lower concentration) and polymer-erosion-controlled release of drug. In this study the erosion of INA was caused by inulinase present in the SCF.

Based on these results it was concluded that INA microparticles would release the loaded drug only upon reaching the colon where colonic bacteria can ferment the inulin and this fermentation will in turn cause drug release by anomalous diffusion of drug from INA microparticles.

4. Conclusion

The present study outlines development of an inulin-based microparticulate colon targeting drug delivery system using electrospraying. Inulin was modified into INA to make it electrosprayable and electrospraying was successfully employed to produce IDM loaded spherical INA microparticles. The encapsulation efficiency of IDM was calculated to be 35.39 ± 1.63% (n = 6). DSC and XRD studies demonstrated that IDM was molecularly dispersed in the INA matrix and remained in an amorphous state ensuring the stability of the developed system. Three-step *in vitro* release study under simulated GI conditions (SGF – 2 h, SIF – 4 h and SCF – 18 h) confirmed that the drug was released only when particles were incubated in inulinase containing SCF. Approximately 60% of the drug was released during 18 h of incubation in SCF. Fitting of IDM release profile to mathematical models indicated that IDM release from INA microparticles was due to a combination of concentration dependent diffusion and polymer erosion controlled release. These results demonstrate that synthesis of INA microparticles for drug delivery by modifying water soluble inulin to make it suitable for electrospraying is a pragmatic approach as this does not compromise the colon targeting ability of inulin.

Acknowledgments

The authors would like to acknowledge the Department of Biotechnology, Government of India for funding this research work; Advanced Center for Material Science and Samtel Center for Display Technologies, IIT Kanpur for providing access to scanning electron microscopy; Central Facility, Chemistry Department, IIT Kanpur for FTIR and NMR spectroscopy; Dr. V. Chandrasekhar and Mr. R. Suriya Narayanan, IIT Kanpur for DSC analysis. DSK acknowledges the 'Batch of 1970 Research Fellowship' received from IIT Kanpur.

Appendix A. Supplementary data

Supplementary data associated with this article can be found, in the online version, at http://dx.doi.org/10.1016/j.carbpol.2014.05.087.

References

Arya, N., Chakraborty, S., Dube, N., & Katti, D. S. (2009). Electrospraying: A facile technique for synthesis of chitosan-based micro/nanospheres for drug delivery applications. *Journal of Biomedical Materials Research Part B: Applied Biomaterials*, *88*(1), 17–31.

Bagheri-Tar, F., Sahimi, M., & Tsotsis, T. T. (2007). Preparation of polyetherimide nanoparticles by an electrospray technique. *Industrial & Engineering Chemistry Research*, *46*(10), 3348–3357.

Bock, N., Woodruff, M. A., Hutmacher, D. W., & Dargaville, T. R. (2011). Electrospraying, a reproducible method for production of polymeric microspheres for biomedical applications. *Polymers*, *3*(1), 131–149.

Bora, M. (2009). *Synthesis and modification of degradable biopolymers for biomedical applications*. Kanpur, India: Department of Biological Sciences and Bioengineering, Indian Institute of Technology Kanpur. Master of Technology thesis

Costa, P., & Sousa Lobo, J. M. (2001). Modeling and comparison of dissolution profiles. *European Journal of Pharmaceutical Sciences*, *13*(2), 123–133.

Davis, S., Hardy, J., & Fara, J. (1986). Transit of pharmaceutical dosage forms through the small intestine. *Gut*, *27*(8), 886–892.

El-Hag Ali, A., & AlArifi, A. (2009). Characterization and in vitro evaluation of starch based hydrogels as carriers for colon specific drug delivery systems. *Carbohydrate Polymers*, *78*(4), 725–730.

Fajardo, A. R., Silva, M. B., Lopes, L. C., Piai, J. F., Rubira, A. F., & Muniz, E. C. (2012). Hydrogel based on an alginate-Ca^{2+}/chondroitin sulfate matrix as a potential colon-specific drug delivery system. *RSC Advances*, *2*(29), 11095–11103.

Franck, A., & De Leenheer, L. (2005). *Inulin*. Biopolymers Online: Wiley-VCH Verlag GmbH & Co. KGaA. Available from: http://dx.doi.org/10.1002/3527600035.bpol6014 [accessed on 17.02.14].

Jaworek, A. (2007). Micro- and nanoparticle production by electrospraying. *Powder Technology*, *176*(1), 18–35.

Jaworek, A., & Krupa, A. (1999). Classification of the modes of EHD spraying. *Journal of Aerosol Science*, *30*(7), 873–893.

Ji, C., Xu, H., & Wu, W. (2007). In vitro evaluation and pharmacokinetics in dogs of guar gum and Eudragit FS30D-coated colon-targeted pellets of indomethacin. *Journal of Drug Targeting*, *15*(2), 123–131.

Jung, J., Arnold, R. D., & Wicker, L. (2013). Pectin and charge modified pectin hydrogel beads as a colon-targeted drug delivery carrier. *Colloids and Surfaces B: Biointerfaces*, *104*, 116–121.

Karavas, E., Georgarakis, E., Sigalas, M. P., Avgoustakis, K., & Bikiaris, D. (2007). Investigation of the release mechanism of a sparingly water-soluble drug from solid dispersions in hydrophilic carriers based on physical state of drug, particle size distribution and drug–polymer interactions. *European Journal of Pharmaceutics and Biopharmaceutics*, *66*(3), 334–347.

McConnell, E. L., Short, M. D., & Basit, A. W. (2008). An in vivo comparison of intestinal pH and bacteria as physiological trigger mechanisms for colonic targeting in man. *Journal of Controlled Release*, *130*(2), 154–160.

Niness, K. R. (1999). Inulin and oligofructose: What are they? *The Journal of Nutrition*, *129*(7), 1402S–1406S.

Poulain, N., Dez, I., Perrio, C., Lasne, M.-C., Prud'homme, M.-P., & Nakache, E. (2003). Microspheres based on inulin for the controlled release of serine protease inhibitors: preparation, characterization and in vitro release. *Journal of Controlled Release*, *92*(1), 27–38.

Seth, A., & Katti, D. S. (2012). A one-step electrospray-based technique for modulating morphology and surface properties of poly (lactide-co-glycolide) microparticles using Pluronics®. *International Journal of Nanomedicine*, *7*, 5129.

Shrivastava, P. K., & Shrivastava, S. K. (2010). Dextran carrier macromolecule for colon specific delivery of celecoxib. *Current Drug Delivery*, *7*(2), 144–151.

Vervoort, L., & Kinget, R. (1996). In vitro degradation by colonic bacteria of inulinHP incorporated in Eudragit RS films. *International Journal of Pharmaceutics*, *129*(1), 185–190.

Wilson, P. J., & Basit, A. W. (2005). Exploiting gastrointestinal bacteria to target drugs to the colon: An in vitro study using amylose coated tablets. *International Journal of Pharmaceutics*, *300*(1-2), 89–94.

Wu, L., Zhang, J., & Watanabe, W. (2011). Physical and chemical stability of drug nanoparticles. *Advanced Drug Delivery Reviews*, *63*(6), 456–469.

Wu, X. Y., & Lee, P. I. (2000). Preparation and characterization of inulin ester microspheres as drug carriers. *Journal of Applied Polymer Science*, *77*(4), 833–840.